Molecular Therapy
Methods & Clinical Development
Original Article

An AAV-SGCG Dose-Response Study in a γ-Sarcoglycanopathy Mouse Model in the Context of Mechanical Stress

David Israeli,[1] Jérémie Cosette,[1] Guillaume Corre,[1] Fatima Amor,[1] Jérôme Poupiot,[1] Daniel Stockholm,[1] Marie Montus,[1] Bernard Gjata,[1] and Isabelle Richard[1]

[1]INTEGRARE, Généthon, INSERM, Université Evry, Université Paris-Saclay, 91002 Evry, France

Sarcoglycanopathies are rare autosomic limb girdle muscular dystrophies caused by mutations in one of the genes coding for sarcoglycans. Sarcoglycans form a complex, which is an important part of the dystrophin-associated glycoprotein complex and which protects the sarcolemma against muscle contraction-induced damage. Absence of one of the sarcoglycans on the plasma membrane reduces the stability of the whole complex and perturbs muscle fiber membrane integrity. There is currently no curative treatment for any of the sarcoglycanopathies. A first clinical trial to evaluate the safety of a recombinant AAV2/1 vector expressing γ-sarcoglycan using an intramuscular route of administration showed limited expression of the transgene and good tolerance of the approach. In this report, we undertook a dose-effect study in mice to evaluate the efficiency of an AAV2/8-expressing γ-sarcoglycan controlled by a muscle-specific promoter with a systemic mode of administration. We observed a dose-related efficiency with a nearly complete restoration of gamma sarcoglycan (SGCG) expression, histological appearance, biomarker level, and whole-body strength at the highest dose tested. In addition, our data suggest that a high expression threshold level must be achieved for effective protection of the transduced muscle, while a suboptimal transgene expression level might be less protective in the context of mechanical stress.

INTRODUCTION

The term sarcoglycanopathies (SGs) comprises four different rare diseases belonging to the larger group of the limb girdle muscular dystrophies (LGMDs): LGMD2C or γ-SG, LGMD2D or α-SG, LGMD2E or β-SG, and LGMD2F or δ-SG. Interestingly, the relative frequency of each form varies enormously between different geographical areas. For example, LGMD2F represents about 14% of SGs in Brazil while being extremely rare elsewhere,[1] and LGMD2C is the almost exclusively occurring form in North Africa and in the Roma populations.[2–5]

LGMD2C is due to mutations in the γ-sarcoglycan (*SGCG*) gene coding for γ-sarcoglycan. SGCG is a single-pass transmembrane glycoprotein with a molecular weight of 35 kDa; it is composed of a small intracellular domain localized on the N terminus, a transmembrane domain and a large extracellular domain, containing N-glycosylation sites. Together with α-, β-, and δ-sarcoglycans, it forms part of the sarcoglycan subcomplex present in the striated muscles. This subcomplex is an important member of the dystrophin-associated glycoprotein complex (DGC), a crucial player in maintaining the linkage between the subsarcolemmal cytoskeleton and the extracellular matrix. Mutations in any of the sarcoglycans perturb the DGC complex formation, leading to a variable level of secondary deficiency of the other sarcoglycans on the sarcolemma. This destabilization of the complex induces a loss of stability in the sarcolemma and a loss of protection of muscle fibers from contraction-induced damage.[6,7]

This loss of protection leads to the genetic defect in LGMD2C inducing a necrotic degenerative-regenerative process, resulting in progressive muscle wasting. The disease is characterized by predominant proximal muscle weakness in the limbs, almost always starting in the lower limbs, common calf hypertrophy, and early joint contractures. The frequency of respiratory insufficiency and dilated cardiomyopathy is variable. Clinical severity is usually correlated with the quantity of residual protein, and genotype-phenotype correlations can be observed. Null mutations are usually associated with absent proteins and severe Duchenne muscular dystrophy (DMD)-like phenotype, while missense mutations are associated with reduced amounts of protein and a milder LGMD-like phenotype.[8,9]

To date, no treatment is available for LMGD2C. Recently, a gene-therapy approach for the correction of the pathology was demonstrated in a mouse model deficient in γ-SG.[10] In 2012, the result of a phase I-II clinical trial for LGMD2C of intramuscular injection of an AAV1 expressing the human γ-SG gene was reported.[11] The results showed good tolerance of the AAV vector with expression of SGCG in all patients but one and the reconstitution of the SG complex. Following this trial, we report here the result of a dose-effect study of the systemic administration of an AAV8 expressing γ-SG under the control of a

Received 17 October 2018; accepted 23 April 2019;
https://doi.org/10.1016/j.omtm.2019.04.007.

Correspondence: Isabelle Richard, INTEGRARE, Généthon, INSERM, Université Evry, Université Paris-Saclay, 1 rue de l'Internationale, 91000 Evry, France.
E-mail: richard@genethon.fr

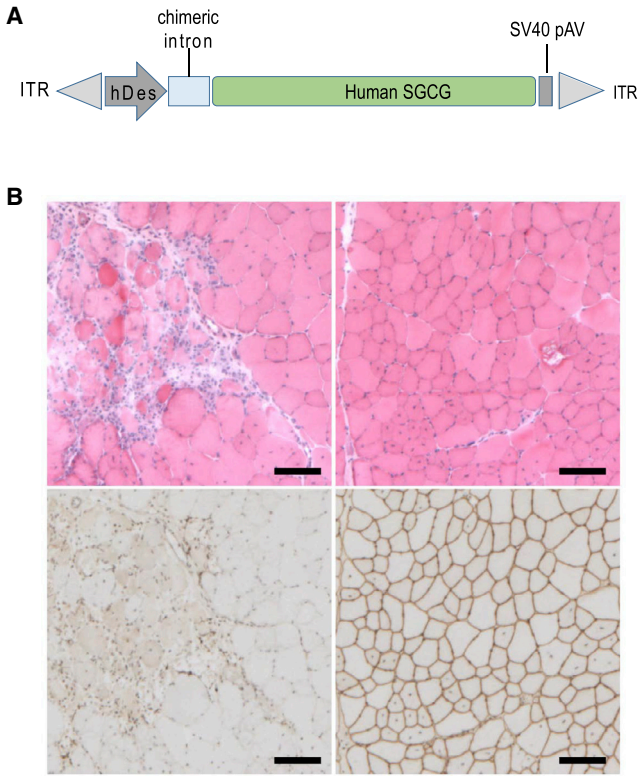

Figure 1. AAV8-desm-hSGCG

(A) Diagram of the AAV vector used in this study. (B) Representative images of H&E staining (top images) and immunostaining for γ-sarcoglycan (bottom images) on transverse sections from non-injected *Sgct*-null (left) and *Sgct*-null mice 1 month after injection of AAV8-desm-hSGCG by intramuscular administration in the tibialis anterior (right). Bar, 100 μm.

muscle-specific promoter in Sgcg$^{-/-}$ mice. Furthermore, we present evidence that in mice undergoing exercise a near-complete transfer must be achieved in order to obtain effective muscle protection.

RESULTS

To evaluate the potential of gene transfer for correcting SGCG deficiency, we produced a rAAV2/8 vector carrying the human *SGCG* cDNA under the transcriptional control of the desmin promoter (Figure 1A). The viral production was validated by intramuscular injection into the tibialis anterior (TA) of 4-week-old male *Sgcg*$^{-/-}$ mice (n = 3 animals per group) with a dose of 1 × 10^{10} viral genome (vg)/TA. After 1 month, muscles were sampled and SGCG expression was determined by immunohistochemistry analysis of transversal sections. While no labeling was observed in *Sgcg*$^{-/-}$ muscles, sampled muscles from the AAV-treated muscles showed widespread staining in nearly 100% of the myofibers with a correct localization on the membrane of the protein associated with a reduction of dystrophic features in histological analysis (Figure 1B). These data validated the functionality of AAV8-desm-hSGCG.

We then performed a dose-response study in *Sgcg*$^{-/-}$ animals. The vector was administered intravenously into the tail vein with three different doses (4.5 × 10^{12}, 1.5 × 10^{13}, and 4.5 × 10^{13} vg/kg) in both male and female 1-month-old animals. Several limb muscles (deltoid, psoas, gluteus, TA, extensorum digitorum longus, gastrocnemius, soleus, quadriceps, triceps crural, heart, and diaphragm) as well as organs (kidneys, lung, liver, spleen) were sampled 1 month after injection (n = 10 per group). Representative images of data obtained after immunolabeling of γ-sarcoglycan on biopsies are presented in Figure 2A. In most of the animals receiving the lowest dose of vector (4.5 × 10^{12}vg/kg), the proportion of γ-sarcoglycan-positive fibers is estimated to be less than 5%. In the group of animals injected with the intermediate dose (1.5 × 10^{13} vg/kg), 25% to 75% of myofibers of the analyzed muscles were shown to be expressed the protein. A level of 75% to 100% positive myofibers was found in most of the muscles injected with the highest dose of vector, 4.5 × 10^{13} vg/kg. The histological analysis also illustrated the dose effect of the vector administration (Figure 2B). A quantitative assessment by western blot analysis of transgene expression in the psoas muscle confirmed the expected dose response (Figures 2C and 2D). A semiquantitative analysis of γ-sarcoglycan expression on the whole-transverse section of the different muscles (left and right sides of the mice) was assessed using a high-throughput method based on ImageJ (see Materials and Methods and Figures S1A and S1B) and is presented in Figure S2A for the females and in Figure S2B for the males, illustrating the dose effect of the administration of the vector. An immunolabeling of serial sections with α- and β-sarcoglycans was also performed and showed a perfect correlation with respect to the presence of the proteins in the different fibers, indicating the reconstitution of the sarcoglycan complex on the sarcolemma in the transduced fibers (Figure 2A).

Quantification of the level of centronucleated fibers and degenerative-regenerative areas of muscle sections corresponding to the different doses injected and controls are represented in Figures 3A and 3B with a score from 0 to 4 (see Materials and Methods). Statistical analyses of these data are presented in Table 1. In the mice injected with the lowest dose of vector (4.5 × 10^{12} vg/kg), all the striated muscles showed various degrees of fiber degeneration. Most of the muscles of the group of mice injected with 1.5 × 10^{13} vg/kg showed low to moderate degrees of dystrophic change. The lowest score of fiber degeneration (score 0) was observed in the animals injected with a high dose of vector (4.5 × 10^{13} vg/kg). No lesion was observed in the histological sections of the hearts of all groups of animals (data not shown). Overall, the percentage of centronucleated myofibers correlated well with the different concentrations of vector injected: the higher the doses, the lower the score of centrally nucleated myofibers. Finally, we performed a functional analysis. All mice were subjected to an escape test at the end of the protocol. The data showed a dose-dependent correction of a deficit in strength in both males and females, with a normalization to the wild-type level only when using the highest dose (Figure 3C). In addition, as a first initial safety evaluation, organs (liver, spleen, lungs, and kidneys) from mice that had previously been injected with a high dose were subjected to histological assessment. Hematoxylin phloxine saffron (HPS) histological observations from different organs showed no significant lesions in animals injected with high doses of vector (data not shown).

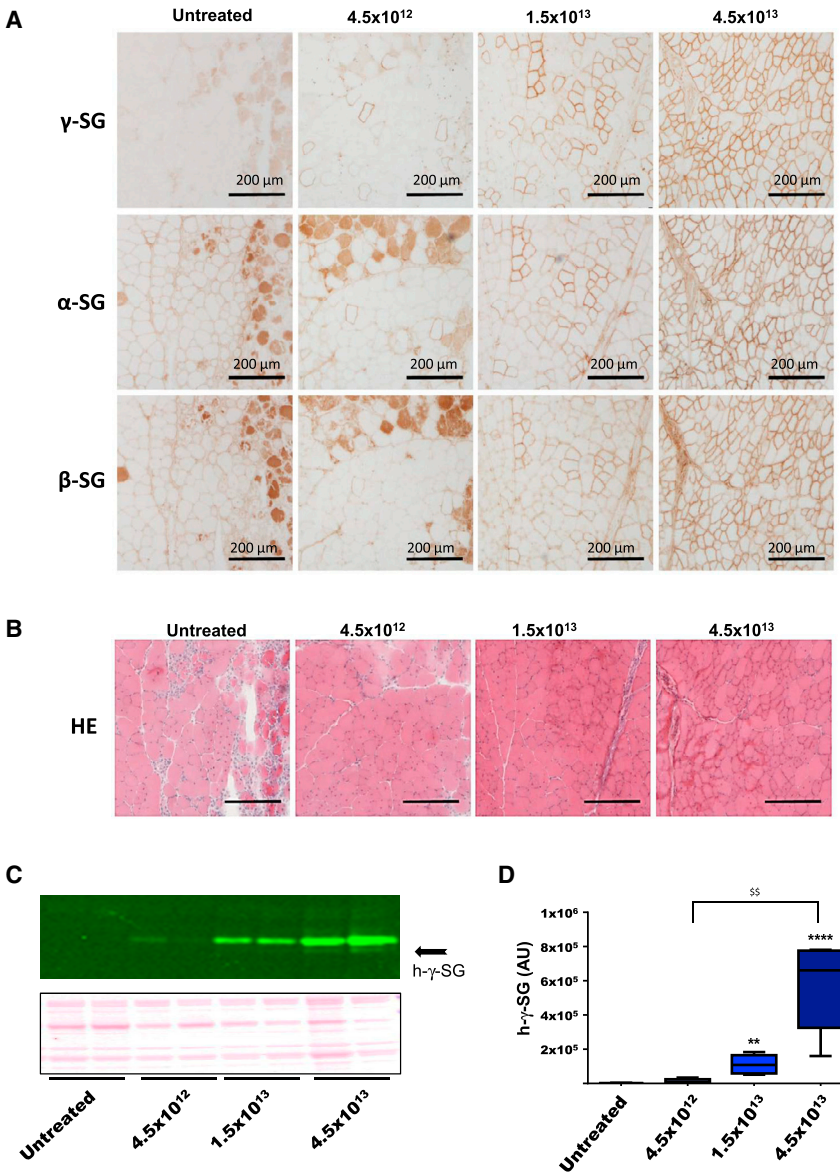

Figure 2. Intravenous Administration of AAV8-desm-hSGCG

(A) Immunolabeling of serial sections of muscles from the anterior compartment (AC = TA + EDL) of the posterior limb after intravenous administration of AAV-SGCG with different doses using antibodies recognizing γ-, α-, or β-sarcoglycans. Bar, 200 µm. Note that a cytoplasmic staining of necrotic fibers is visible in the muscle of untreated and low-titer-treated mice after immunostaining for α- and β-sarcoglycans due to nonspecific binding of the anti-mouse secondary antibody. (B) H&E staining of serial sections. Bar, 200 µm. (C) Western blot detection of human γ-sarcoglycan expression in the psoas muscle of two representative mice, using a human-specific γ-sarcoglycan antibody. (D) Graphical presentation of human γ-sarcoglycan expression in the psoas muscle (n = 8 per group), **p < 0.01, ****p < 0.001, versus the control group, and $$p < 0.01 between groups. See also Figures S1 and S2.

To evaluate the dose effect of the vector injection at a later point and to assess the effect of injection upon exercise, we performed an additional experiment where female mice (n = 10) were injected with the same three doses and analyzed 3 months later. One day before the sacrifice, the mice were subjected to an escape test. Blood sampling was performed at three different time points: at the onset of the experiment, 1 week before the sacrifice, and after the escape test. The histological and functional analyses (Figures 4A, 4B and 4C) confirmed the dose effect of the vector injection seen the previous experience. We evaluated the level of creatine kinase in the serum and also that of dystromiRs (miR-1, miR-133a, mR133b, miR-206, miR-378a-3p, miR-30e, miR-149, and miR-193b). Consistent with our previous studies,[12,13] the serum expression levels of all studied microRNAs (miRNAs) were elevated at the time point D0 (prior to injection) on knockout (KO)-*Sgcg* compared to control healthy mouse (Table S1). In the treated KO-*Sgcg* mice, the serum miRNAs as well as the creatine kinase levels were downregulated in a dose-response manner when analyzed prior to the escape test (Figures 4D and S3). However, we observed a substantially increased level of miRNAs and creatine kinases (CKs) compared to that of the untreated dystrophic group, when measured after the escape test. (Figures 4D and S3). Taken together, these data show that dysregulation of the plasma miRNA profile was reduced in the treated mice for all tested miRNAs, in direct relation to the increased dose of the recombinant vector and transgene expression and with functional recovery of the muscle, where no mechanical stress was involved. In contrast, when mechanical stress was involved, only the mice injected with the highest dose demonstrated a reduction of the miRNA levels compared to the untreated group, suggesting that the muscles must be fully transduced in order to resist better mechanical stress. Interestingly, we observed the occurrence of mosaic fibers that were only partially transduced along their longitudinal axes (Figure 5; Video S1). It is therefore possible that corrected sections of fibers may impose higher mechanical pressure on the untransduced parts.

DISCUSSION

Contrary to the 2012 phase I-II clinical trial for γ-SG sponsored by Généthon, in the present preclinical investigation, we tested an intravenous route of administration and an AAV8-based viral vector for expression of the human γ-sarcoglycan gene. Additional features of the present study were the use of three escalating vector

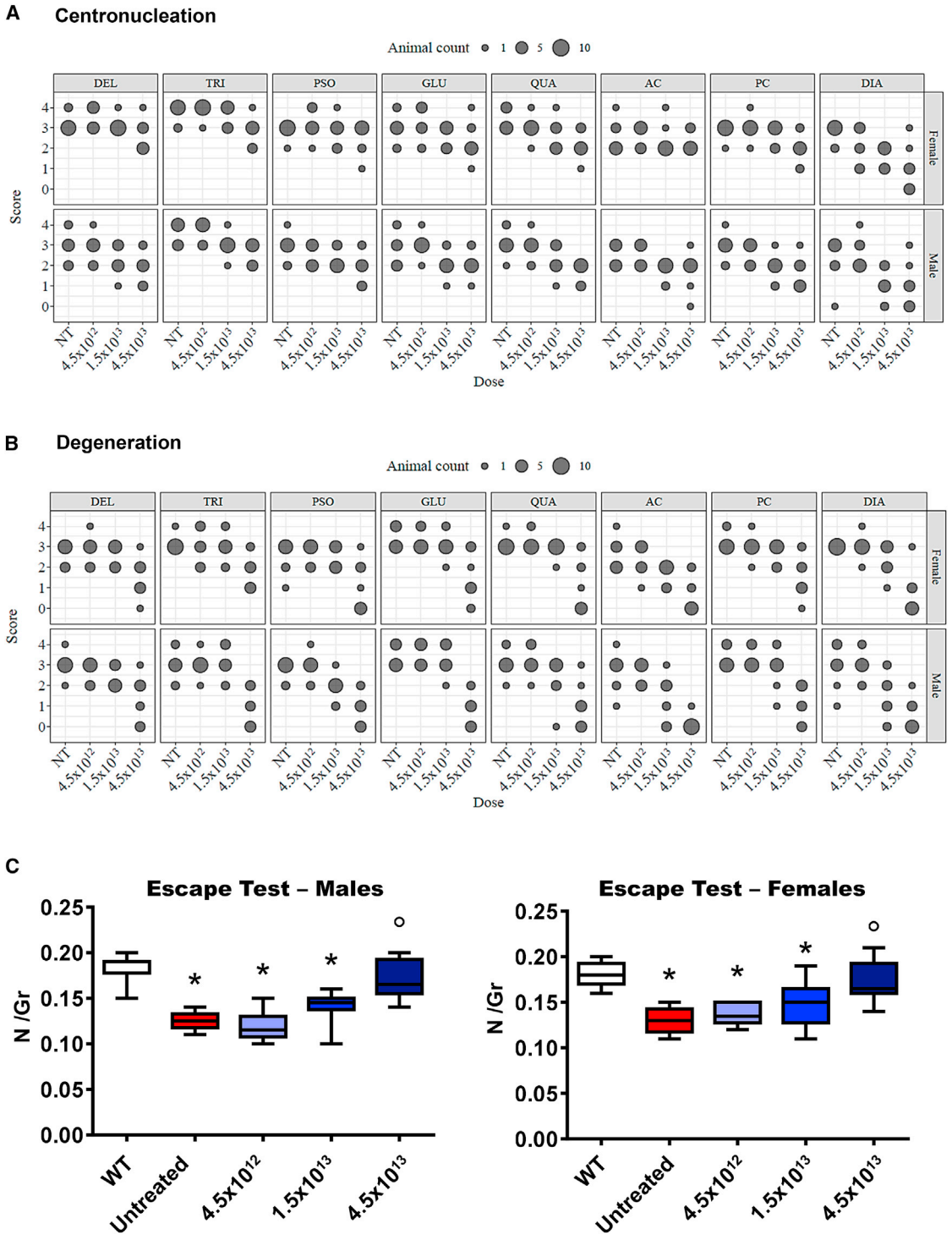

Figure 3. Analyses of the Consequences of AAV8-desm-hSGCG Injection after 1 Month of Injection

(A) Centro-nucleation scoring after the intravenous (i.v.) administration of three doses of AAV8-desm-hSGCG. The size of the dot is proportional to the number of mice presenting a given score, while the scores of 0 to 4 are respectively for up to 5%, 25%, 50%, 75%, and 100% of centro-nucleated myofibers. (B) Degeneration-regeneration

(legend continued on next page)

Table 1. Statistical Analysis for Figure 3

Dose	Sex	DEL	DIA	GLU	AC	PC	PSO	QUA	TRI
Centronucleation									
Untreated	female	CD	D	AB	AB	D	BC	D	CD
Untreated	male	ABCD	CD	AB	AB	CD	BC	CD	BCD
4.5×10^{12}	female	D	BCD	B	B	D	C	BCD	D
4.5×10^{12}	male	ABCD	CD	AB	AB	BCD	ABC	BCD	CD
1.5×10^{13}	female	BCD	ABC	AB	AB	BCD	ABC	ABC	BCD
1.5×10^{13}	male	AB	AB	A	A	AB	AB	ABC	ABC
4.5×10^{13}	female	ABC	A	AB	AB	ABC	ABC	AB	AB
4.5×10^{13}	male	A	A	A	AB	A	A	A	A
Degeneration									
Untreated	female	B	C	B	DE	C	BC	B	B
Untreated	male	B	C	B	E	C	BC	B	B
4.5×10^{12}	female	B	C	B	CDE	C	BC	B	B
4.5×10^{12}	male	B	C	B	DE	C	C	B	B
1.5×10^{13}	female	B	BC	B	BCD	BC	BC	B	B
1.5×10^{13}	male	AB	AB	B	ABC	C	AB	AB	B
4.5×10^{13}	female	A	A	A	AB	AB	A	A	A
4.5×10^{13}	male	A	A	A	A	A	A	A	A

Ordinal regression analysis and Tukey multiple-comparisons summary for Figure 3. For each muscle (columns), conditions (dose and sex) sharing the same letter are not significantly different considering an adjusted p value threshold of 0.05. Centronucleation: for GLU, DEL, and AC, no statistical difference is observed. For all other tissues, only the highest dose shows a significant difference to the untreated group, with the exception of PSO, where the difference is only detected for males. Degeneration: only the highest dose shows a significant difference in the severity score for all tissues. For DIA and AC, a slight improvement is visible with the medium dose. DEL, deltoid; DIA, diaphragm; GLU, gluteus; AC, anterior compartment (tibialis anterior + EDL); PC, posterior compartment (soleus + gastrocnemius); PSO, psoas; QUA, quadriceps; TRI, triceps.

doses, monitoring thus the therapeutic efficiency of gene transfer by extensive histological characterization, muscle function evaluation, and circulating biomarker profiling before and after physical effort.

Compared to AAV1, the AAV8 serotype was reported to have better efficiency in the transduction of striated muscles. The initial clinical trials of neuromuscular diseases were limited to an intramuscular route of administration for safety reasons, but the field is now moving toward systemic administration, thanks to encouraging results from pioneer clinical studies such as the spinal muscular atrophy (SMA) or myotubularin 1 (MTM1) trials (NCT02122952 and NCT03199469). This mode of administration seems mandatory in SGs for reaching therapeutic levels, since the skeletal muscle constitutes approximately 40% of the human body, and some muscles, such as the diaphragm, the intercostal muscles, and the heart, are hardly accessible by intramuscular injections. The extensive histological characterization in our study included both male and female mice, three different vector doses, 10 animals by group, the analysis of eight distinct skeletal muscles and the heart, and quantitative assessment of the sarcoglycan complex and myofiber centronucleation. The human γ-sarcoglycan protein was expressed in all the muscles that were studied and for all the doses that were tested, showing a direct dose-response correlation. Similarly, reduced centronucleation and whole-body force development were proportional to the therapeutic dose. Notably, the strength of the animals treated with the highest dose was no longer significantly different from that of the wild-type (WT) mice. No apparent toxicity has been observed. In conclusion, the intravenous administration of the AAV8-desm-hSGCG product in the γ-sarcoglycan null mouse by systemic route of administration is both safe and efficient. Importantly, the most efficient dose among those tested here was lower than the minimal doses used in the two trials cited above. This observation raises realistic hope for efficiency in future trials for γ-SG.

In addition to defining the dose at the resting state, we were interested in evaluating the efficiency of the gene transfer in the condition of the muscle mechanical challenge that is associated with physical effort. To test this question in the longer term in the γ SG model, we profiled circulating biomarkers in mice that had been treated for 3 months

scoring after the i.v. administration of three doses of AAV8-desm-hSGCG. The size of the dot is proportional to the number of mice presenting a given score, while the scores of 0 to 4 are respectively for up to 5%, 25%, 50%, 75%, and 100% of the muscle section, which corresponds to a degeneration area. Score, max score of left and right muscles per animal. (C) Escape test on male and female, expressed as Newton/Gram (N/Gr). Significance, *$p < 0.05$ versus the wild-type mice. Significance,°$p < 0.05$ versus untreated *Sgcg*-null mice.

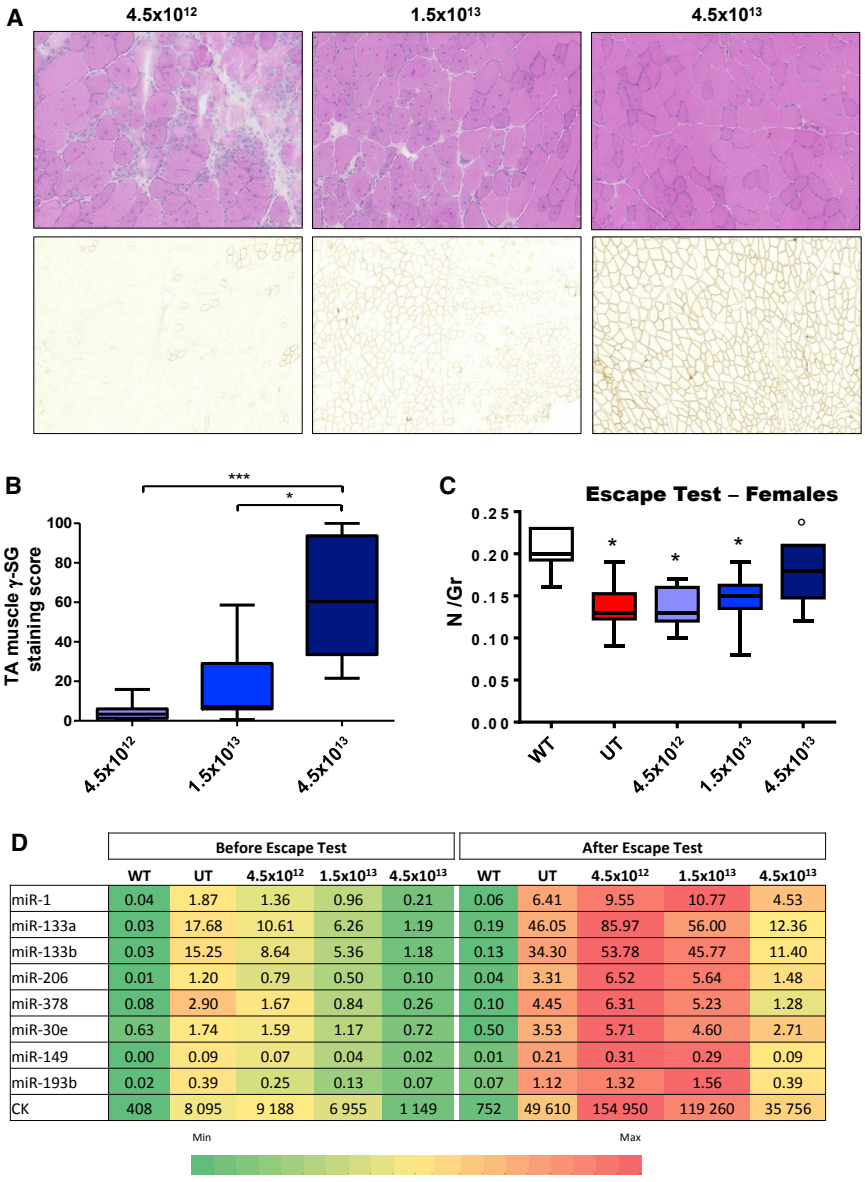

D

	Before Escape Test					After Escape Test				
	WT	UT	4.5x10¹²	1.5x10¹³	4.5x10¹³	WT	UT	4.5x10¹²	1.5x10¹³	4.5x10¹³
miR-1	0.04	1.87	1.36	0.96	0.21	0.06	6.41	9.55	10.77	4.53
miR-133a	0.03	17.68	10.61	6.26	1.19	0.19	46.05	85.97	56.00	12.36
miR-133b	0.03	15.25	8.64	5.36	1.18	0.13	34.30	53.78	45.77	11.40
miR-206	0.01	1.20	0.79	0.50	0.10	0.04	3.31	6.52	5.64	1.48
miR-378	0.08	2.90	1.67	0.84	0.26	0.10	4.45	6.31	5.23	1.28
miR-30e	0.63	1.74	1.59	1.17	0.72	0.50	3.53	5.71	4.60	2.71
miR-149	0.00	0.09	0.07	0.04	0.02	0.01	0.21	0.31	0.29	0.09
miR-193b	0.02	0.39	0.25	0.13	0.07	0.07	1.12	1.32	1.56	0.39
CK	408	8 095	9 188	6 955	1 149	752	49 610	154 950	119 260	35 756

Min Max

Figure 4. Analyses of the Consequences of AAV8-desm-hSGCG Injection upon Mechanical Stress

(A) Histology and immunolabeling of the three doses. Bar, 200 μm. (B) Expression scoring after the i.v. administration of three doses of AAV8-desm-hSGCG in one muscle (TA). Significance: *$p < 0.05$ and ***$p < 0.001$. (C) Escape test, significance (*) is versus the wild-type mice. Significance,°$p < 0.05$ versus untreated *Sgcg*-null mice. (D) Heatmap of miRNA abundance in a pool of serum from all mice per condition (n = 10) before (on the left) and after (on the right) escape test. Note that unlike the miRNA quantification (in a serum pool for each mouse group), the mCK enzymatic activity was performed individually on mice (n = 10). Thus, mCK data on Figure 4D are of average per group, while more detailed results of mCK quantification (including statistics) are presented graphically in Figure S3. miRNA levels are expressed as abundance relative to the average of miR-16, miR-142-3P, and miR-223 of the same sample. CK levels are expressed as enzymatic activity/μL. Color gradient of green to red along the vertical access is for respectively low to high relative miRNA (and mCK) expression levels. See also Table S1.

with escalating doses, before and after the challenge of the muscle function escape test.

Indeed, in the resting mice, tendency toward normalization of the circulating biomarkers (miRNAs + mCK) correlated with the viral dose, while in the mice subjected to the mechanical stress, biomarkers' tendency for normalization was obtained only at the higher viral dose. With lower and intermediate doses, these biomarkers presented in the mechanically stressed mice similar or even increased levels compared to control untreated mice. These results suggest that under conditions of physical effort, a threshold of transgene expression level is required for the stabilization of the myofibers. Of note, a previous study demonstrated that a suboptimal delivery of the AAV-U7ex23 vector for exon skipping in the mdx mouse model for Duchenne muscular dystrophy resulted in the loss of the AAV particles and decreased dystrophin restoration with time.[14] Similarly, a suboptimal dose of sarcoglycan transfer may result in a failure of stabilization of the dystrophic myofibers in the long term, due to loss of the episomal AAV vector. Yet it is not entirely clear why the levels of the circulating biomarkers in the two lower dose groups not only reached, but even exceeded, the levels of the untreated γ sarcoglycan null mice. It is of note that in addition to the fact that the two lower doses resulted in a pattern of transduced fibers surrounded by non-transduced fibers, we also observed that some fibers were only partially transduced along their length, producing a mosaic expression pattern. It is therefore possible that both non-transduced and mosaic fibers were subjected to the damage associated with increased muscle activity or higher shearing forces.

While the dysregulation of circulating miRNAs in muscular dystrophies is well established (reviewed in Coenen-Stass et al.[15]), miRNA profiling for the monitoring of therapeutic efficacy in muscular dystrophy is yet uncommon. Using a mouse model for the α-SG, we previously identified a set of miRNAs that were suited for this purpose.[13] Thus, the present study reinforces the potential utility of this class of biomarkers for therapeutic monitoring in a spectrum of muscular dystrophies. In addition to the well-recognized set of miRNAs dysregulated in muscular dystrophies, (including the

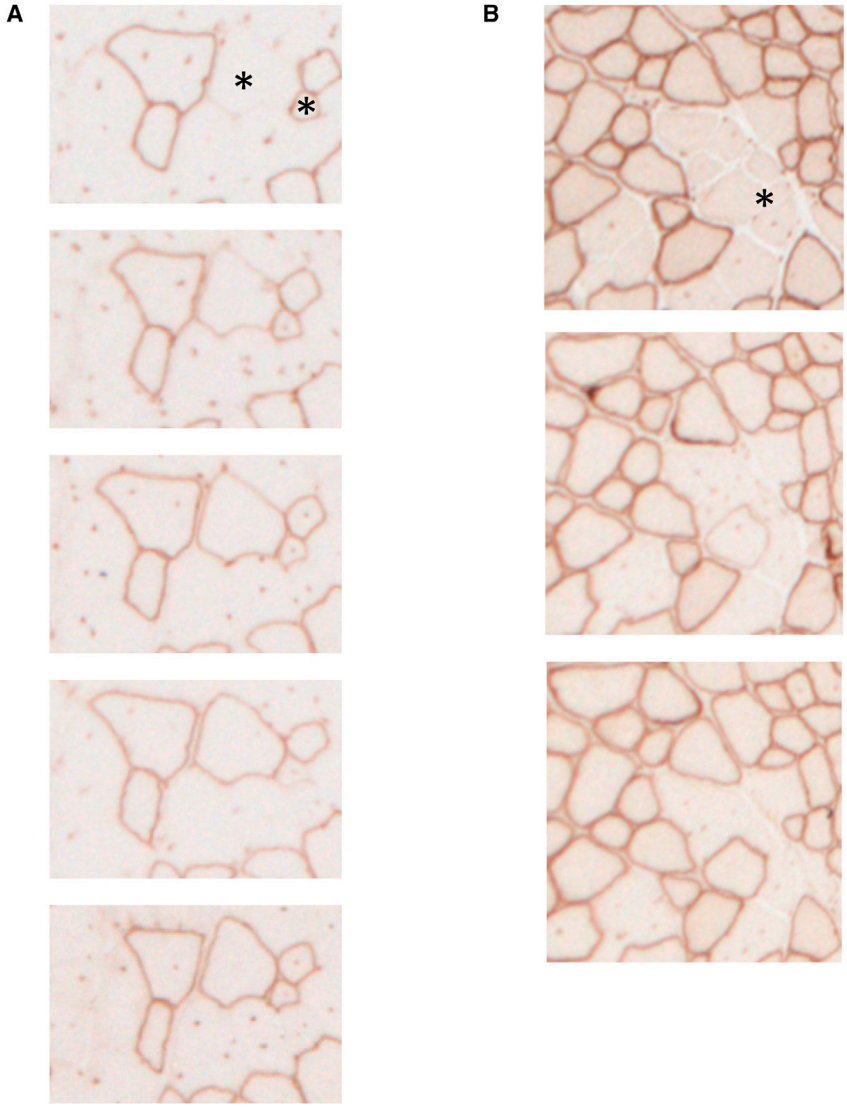

Figure 5. Illustrations of the Partial Transduction of Fibers

(A) Serial sections demonstrated partial transduction along two fibers. See also Video S1. (B) A second example of partial transduction. Asterisks * are inside partially transduced (mosaic) myofibers. See also Video S1.

dystromiRs miR-1, miR-133-a/b, and miR-206), we confirmed here the monitoring potential of miR-30e, miR-149, miR-193b, and miR-378.

Thus, the overall conclusion from the present investigation is that our viral vector might be suited for future clinical trials with human patients. Particular attention and further evaluation of the administrated doses in relation to the threshold expression level of the transgene required for the stabilization of the myofibers under the condition of physical exercise will have to be addressed.

MATERIALS AND METHODS

AAV Construction and Production

The human γ-*SARCOGLYCAN* gene under the control of the desmin promoter (AAV8-desm-hSGCG) was cloned into a donor plasmid (pFastBac) by classical molecular biology technique. Recombinant baculovirus genome was then generated by transposition using the Bac-to-Bac baculovirus expression system. The resulting bacmid DNA was extracted and transfected into insect cells for production of recombinant baculovirus. Baculoviruses harboring the Sgcg cDNA and AAV *rep2/cap8* genes were used to infect spodoptera frugiperda (Sf9) insect cells for production of recombinant adeno-associated virus vector (rAAV). After 72 h of suspension culture at 28°C, the cells were collected by centrifugation and incubated in extraction buffer. Purification was performed on immuno-affinity AVB Sepharose medium (GE Healthcare) according to.[16] Titration was performed by qRT-PCR using primers corresponding to the AAV inverted terminal repeat (ITR).

Animal Care and *In Vivo* Injection

The γ-sarcoglycan ($Sgcg^{-/-}$) mouse model used in this study has been previously described.[17] This model as well as C57Bl6 were bred and housed in a barrier facility with 12-h light, 12-h dark cycles and provided food and water ad libitum. All mice were handled according to the European guidelines for the human care and use of experimental animals, and all procedures on animals were approved by the Généthon's ethics committee under the numbers CE10-122, CE10-123, CE10-124, CE10-127, and CE12-039.

The animals were anaesthetized with a mix of ketamine (100 mg/kg) and xylazine (10 mg/kg). For intramuscular injections, mice were injected into the left TA muscle with a volume of 30 μL. For intravenous injections, a volume of 100 μL/20 g containing the AAV vector was injected into the tail vein. For the duration of the study, all animals were observed twice daily. All animals were weighed on the day of treatment as well as on the day of the necropsy.

Histology and Immunohistochemistry

Skeletal muscles were dissected out and frozen in isopentane cooled in liquid nitrogen. Transverse cryosections (8 μm thickness) were prepared from frozen muscles, air dried, and stored at −80°C. All the other organs were collected and fixed for 24 h in 10% neutral buffered

formalin and embedded in paraffin. H&E staining was performed on all sampled muscles and on liver, lung, kidney, and spleen. Digital images were captured with a CCD camera (Sony). The percentage of centrally nucleated myofibers and the extent of the degeneration area of the muscles were blind scored on H&E-stained muscle sections using the following scale: 0, less than 5% of section; 1, between 5% and 25%; 2, between 25% and 50%; 3, between 50% and 75%; and 4, between 75% and 100%.

Immunostaining for γ-, α-, β-, and δ-sarcoglycan proteins was performed on all sampled muscles. The following primary antibodies were used: goat polyclonal anti-γ-sarcoglycan (D-18) (Santa-Cruz, SC-14180), mouse monoclonal anti-α-sarcoglycan (Novocastra, NCL-a-SARC), and mouse monoclonal anti-β-sarcoglycan (Novocastra, NCL-b-SARC). The sections were treated for 20 min with hydrogen peroxide at room temperature (RT) to inhibit endogenous peroxidases and blocked using the Mouse-on-Mouse kit (Vector Labs). Overnight primary antibody incubations (dilution 1/1,000) were followed by 1 h incubation with horseradish peroxidase (HRP)-conjugated secondary goat antibody and revealed using 3,3′-diaminobenzidine (DAB) solution. Sections were mounted in Eukitt (Orsatech, France) and examined through a Leica confocal microscope (TCS SP2.AOBS microscope, Leica, Germany).

Image Analysis

Images of immunostaining on muscles were acquired using an Axioscan slide scanner (ZEISS, Germany), using a plan-apochromat 10× magnitude 0.45 NA objective. Images of each muscle of each mouse were analyzed using a custom script using ImageJ open-source software.[18] The custom algorithm measures the surface of the transverse sections and the pixel level of the immunolabeling images according to a manually defined threshold to define an index of expression level. The script is available on request. Images were treated with the Enhance Contrast feature and filtered with a variance filter (radius 10 pixels). After being converted into 8-bit and thresholded, the Analyze Particle feature was used to automatically detect the contour of each muscle section. The contouring enables the measurement of complete total surface area of each section. Original images were then converted to 8-bit, and a unique threshold was set by visual validation of fiber detection. This threshold was applied to all images for each different muscle, measuring the sum of pixel intensity corresponding to the labeling. This figure was divided by the surface area of each section. A labeling percentage was then calculated with respect to a treated section with 100% positive fibers that was picked separately for each muscle type as follows: score = number of positive pixels/number of total pixels × 100.

The 3D movie was constructed from 28 sections of 8 μm thick using the plugins Linear Stack Alignment with STIF and 3D viewer of the Fiji software.[19]

Creatine Kinase Analysis

Blood samples were collected by retro-orbital bleeding and quickly centrifuged for 10 min at 8,000 rpm. Sera were harvested and further centrifuged to completely remove cell contaminants. The sera were finally stored at −80°C until measurement. The quantification of mCK activity on individual samples was performed using the Vitros DT60 II Chemistry System according to the manufacturer's instructions (Ortho-Clinical Diagnostics).

miRNA Quantification in Serum

Serum samples were pooled together for each mouse group (n = 10). RNA extraction was performed with the mirVanaTM PARISTM kit (Thermo Fisher). RNA was eluted in 50 μL RNase-free water, concentrated in 10 μL after NaOAc precipitation, and quantified by using a Nanodrop spectrophotometer (ND8000 Labtech, Wilmington, DE, USA). Quantification of miRNAs was performed using Exiqon miRCURY LNA Universal RT microRNA PCR. Total RNA (20 ng) was converted into poly(A) primed universal cDNA, and microRNAs were quantified in duplicate for each sample with miRNA-specific LNA primers on the LightCycler480 (Roche) following the manufacturer's guidelines (miR-133a, miR-133b, miR-1, miR-206, and miR-378). Quantification cycle (Cq) values were calculated with the LightCycler 480 SW 1.5.1 using the 2nd derivative max method. qRT-PCR results, expressed as raw Cq, were normalized to the miRNAs identified as the most stable, miR-16, miR-142-3p, and miR-223. The relative expression was calculated using the $2^{-\Delta\Delta Ct}$ method.

Western Blot Analysis

Frozen sections of approximately 1 mm of the psoas muscle were solubilized in radio immunoprecipitation assay (RIPA) buffer with protease inhibitor cocktail. Protein extract was quantified by BCA (bicinchoninic acid) protein assay (Pierce). 30 μg of total protein were processed for western blot analysis, using an anti-human-specific γ-sarcoglycan antibody (Abcam, ab203112; dilution 1:500). Fluorescence signal of the secondary antibodies was read on an Odyssey imaging system, and band intensities were measured by the Odyssey application software (LI-COR Biosciences, 2.1 version). Ponceau staining was used for the validation of equal protein charge.

Functional Tests

The motor activity of the treated animals was evaluated using the escape test.[20] The procedure follows the recommendations of TREAT NMD SOP for the DMD animal models (http://www.treat-nmd.eu/research/preclinical/dmd-sops/). In brief, mice are placed on a platform at the entrance of a 30-cm-long and 5-cm diameter tube. The animals are connected to a force sensor through their tails. In response to a pinch, the mouse tries to escape and the force generated is recorded. A mean of the five highest scores out of a maximum of 15 during a maximum of 5 min (the first threshold reached) is normalized to the weight of the animal.

Data and Statistical Analysis

The GraphPad PRISM 7.01 program (GraphPad Software, La Jolla, CA, USA) was used for statistics, except for the data in Figures 3A and 3B. The results, which are presented in all the corresponding figures, represent the average ± SEM. Non-parametric ANOVA

(Kruskall-Wallis) tests were used using the Dunnett approach for multiple comparisons (*p < 0.05; **p < 0.01, ***p < 0.005, ****p < 0.001).

Degeneration and centro-nucleation scores in Figures 3A and 3B were analyzed using an ordinal regression (R software v3.5.1 and the ordinal package [https://www.R-project.org/]). The severity score and dose were both treated as qualitative ordinal variables with severity score levels [0 < . . . < 4] and dose levels [UT < lo < med < hi]. A two-way approach is used for each muscle, with dose and sex having 5 and 2 levels, respectively, and using the sex:dose interaction in the model. The significance was tested using a deviance analysis, and post-hoc pairwise comparisons with the Tukey method were then performed to compare groups (full details in the package vignette on CRAN, https://cran.r-project.org/web/packages/ordinal/vignettes/). Statistically different groups (p value < 0.05) are reported with different letters in the summary tables for each score.

SUPPLEMENTAL INFORMATION

Supplemental Information can be found online at https://doi.org/10.1016/j.omtm.2019.04.007.

AUTHOR CONTRIBUTIONS

D.I., M.M., B.G., and I.R. were responsible for the experimental design and project management. J.C. and G.C. developed tools for analysis of the experiments. D.I., J.C., G.C., J.P., and D.S. performed analysis of the data. F.A., J.P., and B.G. performed experiments. D.I., J.P., and I.R. wrote the manuscript.

CONFLICTS OF INTEREST

The authors declare no competing interests.

ACKNOWLEDGMENTS

We would like to thank Alexia Vallet for technical support and to Sian Cronin for critical reading of the manuscript. We are grateful to the "Imaging and Cytometry Core Facility" and the histology team of Généthon for technical support. Equipment funds were from Genopole Research-Evry, University Evry Val d'Essonne, Conseil General de l'Essonne, and from Region Ile de France. Généthon is part of the Biotherapies Institute for Rare Diseases (BIRD), supported by the Association Française contre les Myopathies (AFM-Téléthon).

REFERENCES

1. Moreira, E.S., Vainzof, M., Suzuki, O.T., Pavanello, R.C., Zatz, M., and Passos-Bueno, M.R. (2003). Genotype-phenotype correlations in 35 Brazilian families with sarcoglycanopathies including the description of three novel mutations. J. Med. Genet. *40*, E12.
2. Bönnemann, C.G., Wong, J., Ben Hamida, C., Hamida, M.B., Hentati, F., and Kunkel, L.M. (1998). LGMD 2E in Tunisia is caused by a homozygous missense mutation in beta-sarcoglycan exon 3. Neuromuscul. Disord. *8*, 193–197.
3. Dalichaouche, I., Sifi, Y., Roudaut, C., Sifi, K., Hamri, A., Rouabah, L., Abadi, N., and Richard, I. (2017). γ-sarcoglycan and dystrophin mutation spectrum in an Algerian cohort. Muscle Nerve *56*, 129–135.
4. Piccolo, F., Jeanpierre, M., Leturcq, F., Dodé, C., Azibi, K., Toutain, A., Merlini, L., Jarre, L., Navarro, C., Krishnamoorthy, R., et al. (1996). A founder mutation in the gamma-sarcoglycan gene of gypsies possibly predating their migration out of India. Hum. Mol. Genet. *5*, 2019–2022.
5. Ben Othmane, K., Speer, M.C., Stauffer, J., Blel, S., Middleton, L., Ben Hamida, C., Etribi, A., Loeb, D., Hentati, F., Roses, A.D., et al. (1995). Evidence for linkage disequilibrium in chromosome 13-linked Duchenne-like muscular dystrophy (LGMD2C). Am. J. Hum. Genet. *57*, 732–734.
6. Petrof, B.J., Shrager, J.B., Stedman, H.H., Kelly, A.M., and Sweeney, H.L. (1993). Dystrophin protects the sarcolemma from stresses developed during muscle contraction. Proc. Natl. Acad. Sci. USA *90*, 3710–3714.
7. Cohn, R.D., and Campbell, K.P. (2000). Molecular basis of muscular dystrophies. Muscle Nerve *23*, 1456–1471.
8. Semplicini, C., Vissing, J., Dahlqvist, J.R., Stojkovic, T., Bello, L., Witting, N., Duno, M., Leturcq, F., Bertolin, C., D'Ambrosio, P., et al. (2015). Clinical and genetic spectrum in limb-girdle muscular dystrophy type 2E. Neurology *84*, 1772–1781.
9. Magri, F., Nigro, V., Angelini, C., Mongini, T., Mora, M., Moroni, I., Toscano, A., D'angelo, M.G., Tomelleri, G., Siciliano, G., et al. (2017). The italian limb girdle muscular dystrophy registry: Relative frequency, clinical features, and differential diagnosis. Muscle Nerve *55*, 55–68.
10. Cordier, L., Hack, A.A., Scott, M.O., Barton-Davis, E.R., Gao, G., Wilson, J.M., McNally, E.M., and Sweeney, H.L. (2000). Rescue of skeletal muscles of gamma-sarcoglycan-deficient mice with adeno-associated virus-mediated gene transfer. Mol. Ther. *1*, 119–129.
11. Herson, S., Hentati, F., Rigolet, A., Behin, A., Romero, N.B., Leturcq, F., Laforêt, P., Maisonobe, T., Amouri, R., Haddad, H., et al. (2012). A phase I trial of adeno-associated virus serotype 1-γ-sarcoglycan gene therapy for limb girdle muscular dystrophy type 2C. Brain *135*, 483–492.
12. Vignier, N., Amor, F., Fogel, P., Duvallet, A., Poupiot, J., Charrier, S., Arock, M., Montus, M., Nelson, I., Richard, I., et al. (2013). Distinctive serum miRNA profile in mouse models of striated muscular pathologies. PLoS ONE *8*, e55281.
13. Israeli, D., Poupiot, J., Amor, F., Charton, K., Lostal, W., Jeanson-Leh, L., and Richard, I. (2016). Circulating miRNAs are generic and versatile therapeutic monitoring biomarkers in muscular dystrophies. Sci. Rep. *6*, 28097.
14. Le Hir, M., Goyenvalle, A., Peccate, C., Precigout, G., Davies, K.E., Voit, T., Garcia, L., and Lorain, S. (2013). AAV genome loss from dystrophic mouse muscles during AAV-U7 snRNA-mediated exon-skipping therapy. Mol. Ther. *21*, 1551–1558.
15. Coenen-Stass, A.M.L., Wood, M.J.A., and Roberts, T.C. (2017). Biomarker Potential of Extracellular miRNAs in Duchenne Muscular Dystrophy. Trends Mol. Med. *23*, 989–1001.
16. Smith, R.H., Levy, J.R., and Kotin, R.M. (2009). A simplified baculovirus-AAV expression vector system coupled with one-step affinity purification yields high-titer rAAV stocks from insect cells. Mol. Ther. *17*, 1888–1896.
17. Hack, A.A., Ly, C.T., Jiang, F., Clendenin, C.J., Sigrist, K.S., Wollmann, R.L., and McNally, E.M. (1998). Gamma-sarcoglycan deficiency leads to muscle membrane defects and apoptosis independent of dystrophin. J. Cell Biol. *142*, 1279–1287.
18. Schneider, C.A., Rasband, W.S., and Eliceiri, K.W. (2012). NIH Image to ImageJ: 25 years of image analysis. Nat. Methods *9*, 671–675.
19. Schindelin, J., Arganda-Carreras, I., Frise, E., Kaynig, V., Longair, M., Pietzsch, T., Preibisch, S., Rueden, C., Saalfeld, S., Schmid, B., et al. (2012). Fiji: an open-source platform for biological-image analysis. Nat. Methods *9*, 676–682.
20. Carlson, C.G., and Makiejus, R.V. (1990). A noninvasive procedure to detect muscle weakness in the mdx mouse. Muscle Nerve *13*, 480–484.